Send Orders for Reprints to reprints@benthamscience.net

Micro and Nanosystems, 2021, *13*, 42-48

RESEARCH ARTICLE

A Discussion Regarding the Application of the Hertz Contact Theory on Biological Samples in AFM Nanoindentation Experiments

Stylianos Vasileios Kontomaris[1,2,*], Andreas Stylianou[3], Konstantina S. Nikita[1] and Anna Malamou[4]

[1]*Mobile Radio Communications Laboratory, School of Electrical and Computer Engineering, National Technical University of Athens, Athens, Greece;* [2]*Faculty of Architecture, Engineering & Built Environment, Athens Metropolitan College, Athens, Greece;* [3]*Cancer Biophysics Laboratory, Department of Mechanical and Manufacturing Engineering, Faculty of Engineering, University of Cyprus, Nicosia, Cyprus;* [4]*Radar Systems and Remote Sensing Lab of School, Electrical & Computer Engineering, National Technical University of Athens, Athens, Greece*

ARTICLE HISTORY

Received: August 07, 2019
Revised: November 11, 2019
Accepted: December 29, 2019

DOI:
10.2174/1876402912666200115160207

Abstract: ***Background*:** Atomic Force Microscopy (AFM) Nanoindentation procedure regarding biological samples poses significant challenges with respect to the accuracy of the provided results. These challenges are related to the inhomogeneity of biological samples, various uncertainties in experimental methods and certain approximations regarding the theoretical analysis. The most commonly used theoretical model for data processing at the linear elastic regime regarding biological samples is the Hertz model.

***Objective*:** This paper focuses on the investigation of the resulting errors of the basic equation of the Hertz theory that depend on the ratio, indentation depth/indenter's radius regarding the Young's modulus calculation.

***Methods*:** An extended new equation is derived which takes into account the influence of the indentation depth/indenter's radius ratio on the calculation of the Young's modulus and can be easily used for calculations. The derived equation is further combined with equations which take into account the shape of the sample.

***Results*:** Several examples in the literature that do not take into account the value of the ratio indentation depth/indenter's radius are reported and the related errors are calculated and discussed. Moreover, a rational explanation, regarding the extended differences of the Young's modulus calculations using the same experimental results when these are processed using the Hertz model and the Oliver & Pharr analysis (which is the general model that applies for any axisymmetric indenter) is provided.

***Conclusion*:** A complete and reliable theoretical tool was developed (that takes into account the indentation depth/indenter's radius ratio and the shape of the sample) which can be generally applied in order to reduce the errors produced by the current methodology (Hertz model).

Keywords: Mechanical properties, hertz model, biological samples, Atomic Force Microscopy (AFM), nanoindentation, indentation values.

1. INTRODUCTION

The theory related to the interaction between two solids is of great value to the scientific fields of nanotechnology, biophysics and biological sciences [1]. More specifically, this theory is used in a wide range of nanotechnology-based applications and procedures, ranging from imaging at the nanoscale to the nanomechanical characterization of samples and bio-samples [2-6]. The nanomechanical characterization can be performed using state of the art equipment such as Atomic Force Microscopy (AFM) [7-11]. The basic property of a material which can be calculated with AFM is the Young's modulus of the sample of interest [1]. The Young's modulus (Young's modulus is a measure of the stiffness of an elastic material, and it is defined as the ratio of stress to strain) can be calculated using several models arising from the contact mechanics theory depending on the indenter's shape (*e.g.* the shape of the AFM tip) and the shape of the sample [12, 13]. Towards this direction, in a typical nanoindentation experiment, the mechanical response of a sample is tested using the AFM tip. In particular, the tip is used in order to achieve a specific value of applied load and subsequently, the indentation is calculated (the indentation can be easily calculated from the difference between the piezo-displacement for a hard reference sample and the soft sample in order to succeed the same deflection of the cantilever) [1, 11, 14]. Based on the applied load and the indentation values on a specific point of a sample, a load – indentation curve is constructed. Using this curve, the Young's modulus can be easily determined as a fitting parameter [15].

In the field of biological samples and biomaterials, the most widely applied model for data processing is the Hertz model that can only be applied under specific restrictions [16]. Firstly, the tested sample must be isotropic (*i.e.* the

*Address correspondence to this author at the Mobile Radio Communications Laboratory, School of Electrical and Computer Engineering, National Technical University of Athens, Greece; and Athens Metropolitan College, Athens, Greece; Tel: 6978886579;
E-mail: skontomaris@mitropolitiko.edu.gr

properties of the material are the same in all directions) and homogeneous (*i.e.* the material has uniform composition and uniform properties throughout) [16]. Despite the fact that biological samples at the nanoscale do not follow these requirements, several approximations can be used. For example, a sample can be considered as an elastic half-space when the indenter's size is significantly smaller as compared to the dimensions of the sample and the indentation depths are small (an elastic half-space is an isotropic and homogeneous material that is assumed to extend infinitely in all directions and in-depth, with the top surface as a boundary). In addition, the contact between the tip and the sample must be adhesionless and frictionless [17-19]. This requirement is difficult to be valid unless the sample is tested in a liquid environment. Furthermore, according to Buckle's rule, the indentation depth cannot exceed 5-10% of the sample's thickness [14, 20], while the contact geometry must be axisymmetric, smooth and continuous [5]. Under the aforementioned requirements, the data related to nanoindentation experiments on biosamples (such as cells, proteins, articular cartilage, *etc*.) can be processed using the equation provided by the Hertz contact mechanics which relates the applied load to the indentation depth (the requirements in order to apply the Hertz model are presented in Table **1**). In particular,

$$P(h) = \frac{4E}{3(1-v^2)}\sqrt{R}h^{3/2} \quad (1.1)$$

In Eq. (1.1), P is the applied load, h is the indentation depth, R is the indenter's radius, E and v are the Young's modulus and the Poisson's ratio of the sample, respectively $(0 \leq v \leq 0.5)$ [15].

The basic procedure is to fit the load – indentation data to equation (1.1) and calculate the Young's modulus as a fitting parameter (under the condition that the indenter's radius and the Poisson's ratio of the sample are known) [15]. Eq. (1.1), is widely used in the literature, however, it is based on a basic approximation which is h<<R [6, 21]. In particular, if h<<R, the contact radius between a spherical indenter and an elastic half-space is given by the equation [22]:

$$r_c = \sqrt{2Rh_c} \quad (1.2)$$

In Eq. (1.2), h_c is the depth at which contact is made between the indenter and the sample during indentation (Fig. **1**). Equation (1.2) provides approximately the contact radius and this approximation is taking into account for deriving Eq. (1.1) [16]. As a consequence, the generally used Eq. (1.1) is valid only under the assumption that (1.2) provides an approximately correct value for the contact radius. However, according to the Oliver – Pharr analysis in the case of a perfect spherical indenter, the contact radius is given by the following extended equation [6, 23]:

$$r_c = \sqrt{2Rh_c - h_c^2} \quad (1.3)$$

Usually, it is considered that $h_c^2 \ll 2Rh_c$ which is a rational approach in many cases ($h_c < h$ and as a result, this assumption is valid in cases that the indentation depth is significantly smaller than the indenter's radius). In a real nanoindentation experiment, a logical relation between h and R is h<R/10 as it is presented by Radmacher, 2007 [21]. Hence, in the case that the indentation depth is significantly smaller than the indenter's radius, Eq. (1.3) is approximately equal to Eq. (1.2) and as a result, Eq. (1.1) can be used for the Young's modulus calculation. In this paper, we explore the range of values h/R which leads to negligible errors when using the Eq. (1.1) for the Young's modulus calculation. In addition, a discussion regarding the rationality of the above-mentioned assumption is presented.

2. THEORETICAL ANALYSIS AND EXPERIMENTAL RESULTS: MATERIALS AND METHODS

2.1. Theoretical Investigation of the Errors Arising for Big h/R Ratios

As it has been proven by Oliver & Pharr, the Young's modulus of a sample in an AFM nanoindentation experiment can be calculated using the following equation which can be applied for any axisymmetric indenter [5]:

$$E = \frac{\sqrt{\pi}}{2}(1-v^2)\frac{S}{\sqrt{A}} \quad (2.1)$$

where, E is the Young's modulus, v is the sample's Poisson's ratio, S is the contact stiffness, and A is the effective cross-sectional or projecting area of the indenter. The contact stiffness can be determined by the slope of the upper unloading part of the load-indentation curve, thus [6, 14]:

$$S = \frac{dP}{dh}, \text{(at the inception } h = h_{max}) \quad (2.2)$$

By substituting equation (2.2) to equation (2.1), we derive the following expression:

$$\frac{dP}{dh} = \frac{2E}{\sqrt{\pi}(1-v^2)}\sqrt{A} \quad (2.3)$$

In the case of a nanoindentation experiment using a spherical indenter with radius R, the cross-sectional area can be calculated as follows [23]:

$$A = \pi r_c^2 = \pi(2Rh_c - h_c^2) \quad (2.4)$$

Table 1. Requirements for the application of the Hertz contact theory.

Requirements for the Application of the Hertz Model in Nanoindentation Experiments
The sample is flat, isotropic and homogeneous
The contact between the tip and the sample is adhesionless and frictionless
The contact geometry is assumed to be axisymmetric, smooth and continuous
The indentation depth cannot exceed the 5-10% of the sample's thickness (Buckle's rule)

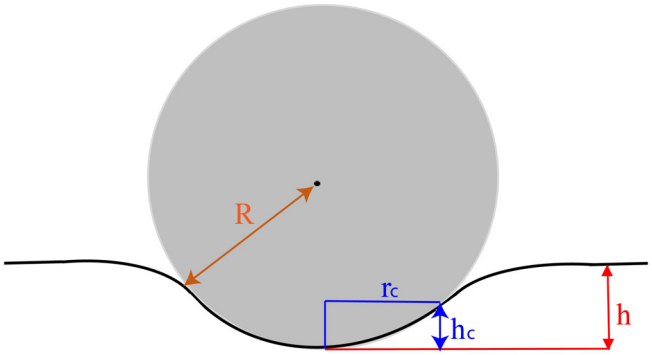

Fig. (1). An illustration of a nanoindentation experiment using a spherical indenter. The magnitudes R, h_c, r_c and h are clearly presented. (*A higher resolution / colour version of this figure is available in the electronic copy of the article*).

In Eq. (2.4), h_c is the depth at which contact is made between the indenter and the sample during indentation. By combining equations (2.3) and (2.4), we derive:

$$\frac{dP}{dh} = \frac{2E}{(1-v^2)}\sqrt{(2Rh_c - h_c^2)} \tag{2.5}$$

Equation (2.5) can be modified as follows:

$$\frac{dP}{dh} = \frac{2E}{(1-v^2)}\sqrt{2Rh_c\left(1-\frac{1}{x}\right)} \tag{2.6}$$

Where, $h_c^2 = \frac{2Rh_c}{x}$, x>0 and as a result, x=2R/h_c (x is a constant parameter for a specific nanoindentation experiment). In addition, according to Oliver & Pharr analysis, the contact depth is calculated by the following equation [6, 14, 23]:

$$h_c = h_{max} - \varepsilon\frac{P_{max}}{S} \tag{2.7}$$

where ε is a constant that depends on the geometry of the indenter. Furthermore, the applied load during indentation is related to the contact depth by the following equation [15]:

$$P = ah^m \tag{2.8}$$

In Eq. (2.8), the coefficients *a*, m can be easily determined as fitting constants. The coefficients ε, m are related to the equation [6, 23, 24]:

$$\varepsilon = m\left[1 - \frac{2\Gamma\left(\frac{m}{2(m-1)}\right)(m-1)}{\sqrt{\pi}\Gamma\left(\frac{1}{2(m-1)}\right)}\right] \tag{2.9}$$

In Eq. (2.9), Γ is the Gamma function. Using Eq. (2.8), the contact stiffness (Eq. 2.2) can be written in the form:

$$S = amh_{max}^{m-1} = mP_{max}h_{max}^{-1} \tag{2.10}$$

The above-mentioned equation (2.10) can be also written in the alternative form:

$$\frac{P_{max}}{S} = \frac{h_{max}}{m} \tag{2.11}$$

Using Eq. (2.11), the contact depth results in:

$$h_c = h_{max}\left(1-\frac{\varepsilon}{m}\right) \tag{2.12}$$

Hence, the differential equation (2.3) takes the simple form:

$$\frac{dP}{dh} = b\sqrt{h} \tag{2.13}$$

Where, the coefficient *b* is given by the following equation:

$$b = \frac{2E}{1-v^2}\sqrt{2R\left(1-\frac{\varepsilon}{m}\right)\left(1-\frac{1}{x}\right)}$$

The solution of the differential equation provided by Eq. (2.13) is presented below:

$$P(h) = \frac{2}{3}bh^{3/2} + c_1 \tag{2.14}$$

However, in a nanoindentation experiment of h=0, P(h)=0, thus c_1=0. As a result, the equation which relates the applied load and the indentation depth in an experiment using a spherical indenter is the following:

$$P(h) = \frac{4E}{3(1-v^2)}\sqrt{2R\left(1-\frac{\varepsilon}{m}\right)\left(1-\frac{1}{x}\right)}h^{3/2} \tag{2.15}$$

By combining Eqs. (2.8) and (2.15), we conclude that in the case of a nanoindentation experiment using a spherical indenter, m=3/2. In addition, using Eq. (2.9) we conclude in ε=0.75 for spherical indentations. Thus,

$$P(h) = \frac{4E}{3(1-v^2)}\sqrt{R}h^{3/2}\sqrt{1-\frac{1}{x}} \tag{2.16}$$

In the case that $x \to \infty$ (*i.e.* $\frac{h_c}{R} \to 0$), we derive the classic approximate solution for a spherical indentation:

$$P(h) = \frac{4E}{3(1-v^2)}\sqrt{R}h^{3/2} \tag{2.17}$$

Using the values m=1.5 and ε=0.75 we conclude that (since x=2R/h_c):

$$x = \frac{4R}{h_{max}} \tag{2.18}$$

Following the above, we will investigate the errors arising for indentation depth values (using spherical indenters) in the range:

$$\frac{R}{20} \le h_{max} \le \frac{2R}{3} \tag{2.19}$$

Indentation depths in the range indicated by Eq. (2.19) are common in the literature as it will be discussed in the 'Discussion' section. As a result,

$$80 \ge x \ge 6 \tag{2.20}$$

The equation which relates the Young's modulus using the approximation $x \to \infty$ (h<<R), E_a and the real Young's modulus E_r is presented as follows:

$$\frac{E_r}{E_a} = \left(1-\frac{1}{x}\right)^{-\frac{1}{2}} \tag{2.21}$$

A graphical representation of Eq. (2.21) is shown in (Fig. **2**). For the range of values h/R provided by Eqs. (2.19), (2.20) the ratio E_r/E_a results in:

$$1.0063 \le \frac{E_r}{E_a} \le 1.095 \tag{2.22}$$

Eq. (2.22), indicates that the percentage difference between the real Young's modulus value E_r and the approximated value E_a is 0.63% if h=R/20 and 9.5% of h=2R/3. The proposal provided by Radmacher [21] [(*i.e.* that (1.1)

can be used if h<R/10) is rational since in this case $\frac{E_r}{E_a} = 1.0127$, thus the real value is only 1.27 % bigger comparing to the approximate value].

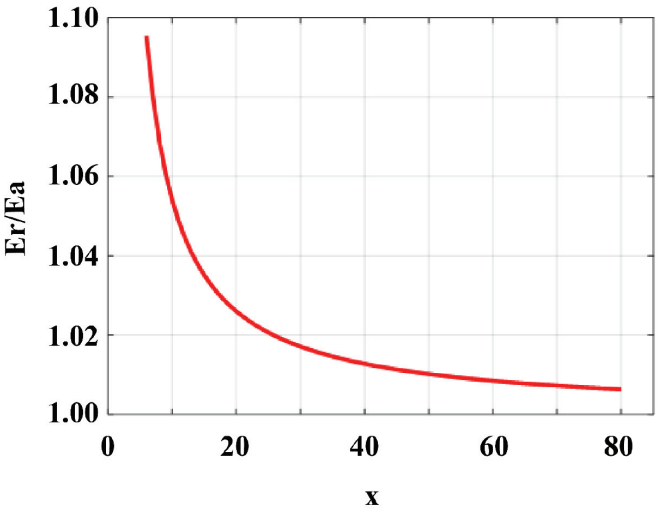

Fig. (2). The variation of the ratio Er/E_a with respect to x. In the case that x=6, h/R=2/3 and Er/Ea=9.5. In addition, in the case that x=80, h/R=1/20 and as a result Er/Ea=1.0063. (*A higher resolution / colour version of this figure is available in the electronic copy of the article*).

2.2. Investigation and Determination of the Arising Errors in a Real Nanoindentation Experiment

A typical load – indentation curve obtained on an H4 human glioma cell is presented in (Fig. **3**). The nanoindentation experiment was performed using an indenter with a radius equal to R=2.5 μm. In this experiment, the maximum indentation depth was equal to 1.014 μm. As a result, h/R=0.41 and x=9.76. In this case, E_r/E_a =1.055 and the real Young's modulus value is 5.5 % bigger comparing to the approximated value. Thus, using Eq. (1.1), we conclude that E_a=1.07 kPa. This value is based on the assumption (h<<R). However, using the extended Eq. (2.16), provided by this paper, we calculate E_r=1.13 kPa, which is the correct value for the Young's modulus. Details regarding the nanoindentation experiments and data processing are also presented in the Appendix.

3. RESULTS AND DISCUSSION

As it has been already mentioned in the introduction, the Hertz model is probably the most widely used contact mechanics model used in experiments regarding biological samples and biomaterials with regards to the Young's modulus calculation. Eq. (1.1) is usually used for fitting the experimentally obtained data in order to determine the Young's modulus of the sample of interest. However, as it was presented in this paper, the use of Eq. (1.1) could probably induce errors in the analysis depending on the ratio h/R. Thus, we presented an extended equation which relates the Young's modulus value to the ratio h/R. Despite the fact that empirically obtained findings are provided in the literature (*e.g.* the assumption provided by Radmacher, 2007 [21], h/R<10) in this paper, an extended analysis was performed which justifies the Radmacher assumption and provides an extended discussion regarding the resulting errors that arise by using the Eq. (1.1). In addition, an accurate equation (Eq. 2.16), which depends on the ratio h/R was presented that can be used for an accurate fitting procedure to avoid the underestimation of the Young's modulus value.

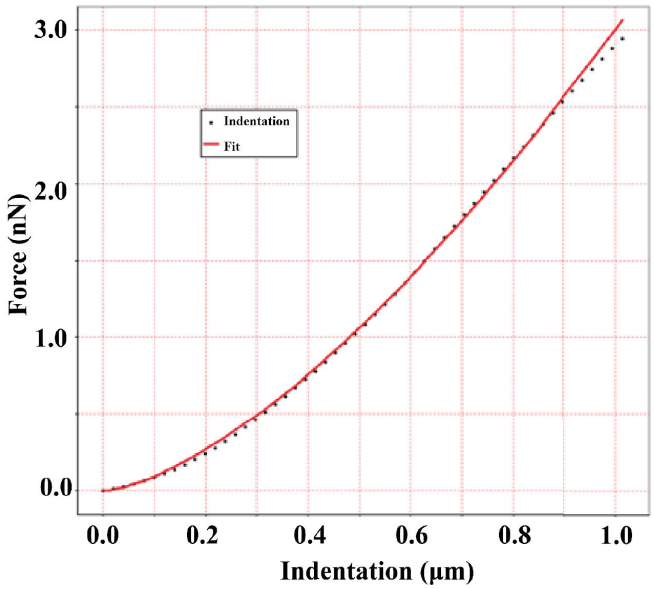

Fig. (3). A typical load – indentation curve obtained on a H4 human glioma cell. The nanoindentation experiment was performed using an indenter with radius equal to R=2.5 μm. In this experiment the maximum indentation depth was equal to 1.014 μm. As a result, h/R=0.41 and x=9.76. Thus, the arising error using Eq. (1.1) results in 5.5 %. The fitting was performed using the Atomic J software. (*A higher resolution / colour version of this figure is available in the electronic copy of the article*).

It is a fact that Eq. (1.1) is usually used without taking into consideration the relationship between the indenter's radius and the indentation depth. Many examples can be found in the literature. In particular, Guo *et al.*, 2014 performed nanoindentation experiments on cancerous and non-cancerous human mammary epithelial cells. In their experiments, they used a 2.65 μm radius spherical tip [25]. The indentation depth for all the experiments was selected equal to 1500 nm. As a result, h/R=0.57 and x=7.067. Thus, the resulting error is 7.93 %. Shimizu *et al.* 2012 performed nanoindentation experiments to measure the Young's modulus of mesenchymal stem cells and HEK293 cells in the floating state [26]. For the Young's modulus determination, a modification of Eq. (1.1) was used which takes into account the spherical shape of the cell. In particular, the effective radius was used which is equal to $R^*=R_1R_2/(R_1+R_2)$, where R_1 is the radius of the spherical probe and R_2 the cell's radius. The nanoindentation depths presented in this paper were in the range 1 μm – 2.5 μm. In addition, R_1=2 μm and R_2=7.5 μm for the hMESC and R_2'= 6.6 μm for the HEK 293. For the case of an hMEC cell R*=1.58 μm. Thus, for an indentation depth equal to 1 μm, h/R*=0.63, x=6.33 and the resulting error in the Young's modulus calculation is approximately 9.0 %. In addition, for a HEK 293 cell, R*=1.53 μm, h/R*=0.65 and x=6.15. Hence, the resulting

error is approximately 9.3 %. It is obvious that for h>1 μm the errors are significant and major miscalculations regarding the Young's modulus have been observed. Moreover, Grant *et al.* 2009 used the AFM nanoindentation method to determine the mechanical properties of hydrated collagen fibrils [27]. They used the modification of Eq. (1.1) for the contact problem of sphere-cylinder interaction (*i.e.* $R'=R_1R_2/(R_1+R_2)$ where R_1 is the radius of the spherical probe and R_2 the cylinder's radius. As it is reported in their work, Eq. (1.1) can be used for a spherical or a parabolic probe. However, they used high indentation depths, up to $5\times R_{tip}$. According to our analysis, this fact leads to a significant underestimation of the Young's modulus. Furthermore, Sajeesh *et al.*, 2016 used Eq. (1.1) to calculate the Young's modulus of fibroblasts [28]. In their experiments, they used a spherical probe with radius equal to 5 μm and maximum indentation depth 1000 nm (*i.e.* h/R=0.2). In this case, x=20 and the resulting error is small, 2.6 %.

An interesting analysis regarding the mechanical properties of murine collagen fibrils is presented by Andriotis *et al.,* 2014 [29]. In their analysis, they performed a comparative analysis for the determination of the Young's modulus, using Eqs. (1.1) (approximate Hertz model) and (2.1) (Oliver and Pharr analysis). Using the modified Hertzian contact model for the sphere – cylinder interaction, the Young's modulus of the fibrils resulted in 6.9±1.3 GPa. However, using the Oliver & Pharr analysis, the result was significantly bigger, *i.e.* 9.3±1.3 GPa. In addition, it must be reported that statistical analysis showed significant differences (P-value <0.05) between the Oliver–Pharr and the Hertzian analysis (P-value=0.02). Despite the fact that our analysis explains up to a level the difference in the Young's modulus value (by using either the Hertz model or the Oliver-Pharr analysis), it seems that it is not the only factor that influenced this result. More specifically, the difference as it was calculated by Andriotis *et al.,* 2014 analysis between the two approaches was ~ 34 %. This difference indicates that there are more factors responsible for deviations regarding the Young's modulus calculations using the aforementioned approaches. However, our analysis provides a rational factor that explains this difference up to a level. It seems that the Oliver-Pharr analysis provides more accurate results in this case (comparing to the Hertz model) since for the Young's modulus calculations it takes into account Equation (1.3) instead of (1.2).

The Young's modulus calculations regarding biological samples is a challenging procedure. A variety of biosamples have been investigated using AFM by many researchers in different laboratories. As a consequence, a significant number of papers that concern the mechanical properties of biological samples have been published. However, the aforementioned papers present significant variations in the provided values, even for the same biological tissue. These variations can be related to two main sources: biological variability and technical inaccuracy. An interesting biological sample with an extended range of Young's modulus values in the literature is collagen. In particular, Heim *et al.*, 2006 concluded that the Young's modulus of individual collagen fibrils is in the range 1 – 2 GPa [30]. In the same order of magnitude are also the results provided by Grant *et al.*, 2009 (1.9±0.5) GPa [27]. On the contrary, Wenger *et al.*, 2007 concluded in a significantly bigger range of values: 5 GPa – 11.5 Gpa [23]. An interesting fact is that the results provided by Grant *et al.*, 2009 and Heim *et al.*, 2006 were about 7 times smaller compared to the results provided by Wenger *et al.*, 2007 even though all these experiments focused on type I collagen fibrils (however, the samples were provided from different species) [23, 27, 30]. Significant research efforts have been performed in the previous years to explain the aforementioned differences. For example, a possible explanation could be related to the variation of the cross-linking. Apart from biological reasons, Andriotis *et al.*, 2014 proved that the model that is used for the contact mechanics analysis results in significant differences regarding the Young's modulus calculations [29]. In this paper, we provide an explanation that up to a level explains the dependence of the calculated values from the used model. This research is a step forward towards the development of significant theoretical tools to minimize the dependence of the results on the model used in the data processing. However, more research is needed in order to provide a complete explanation regarding the differences provided by the Hertz model and the Oliver-Pharr analysis since our proposal explains it up to a certain level.

Previous studies presented the resulting errors which arise from the consideration of a cylindrical/spherical sample as a half-space [12]. This analysis concluded that Eq. (1.1) can be modified for the case of cylindrical samples:

$$P(h)=\frac{4E}{3(1-\nu^2)}\sqrt{R}h^{3/2}Z \tag{3.1}$$

Where Z is a correction factor which expands the applicability of Eq. (1.1) to cylindrical samples.

In addition, Eq. (1.1) can be also modified for spherical samples as follows:

$$P(h)=\frac{4E}{3(1-\nu^2)}\sqrt{R}h^{3/2}Q \tag{3.2}$$

Where Q is the correction factor which expands the applicability of Eq. (1.1) to spherical samples. These results can be combined with the analysis provided in this paper to develop an equation which takes into account both the shape of the sample and the dependence on h/R ratio. Thus, for cylindrical shaped samples, we conclude that:

$$P(h)=\frac{4E}{3(1-\nu^2)}\sqrt{R}h^{3/2}Z\sqrt{1-\frac{1}{x}} \tag{3.3}$$

In addition, for a spherical shaped sample:

$$P(h)=\frac{4E}{3(1-\nu^2)}\sqrt{R}h^{3/2}Q\sqrt{1-\frac{1}{x}} \tag{3.4}$$

An interesting point regarding collagen (which can be modeled as a cylinder-shaped sample) is that the consideration of a fibril as a half-space combined to a high ratio of h/R could result in a significant error in the analysis. For example, under the assumption $R_t/R_c=0.3$ where R_t is the indenter's radius and R_c the cylinder's radius and $h/R_c=0.5$ we conclude that Z=1.066 [12] and x=8. Hence, the deviation of the Young's modulus value [calculated from Eq. (1.1)] from the actual value [calculated from Eq. (3.3)] is approximately 14 %. This result proves the significance of the research concerning the improvement of models of applied mechanics that are being used in AFM nanoindentation experiments on biological samples.

4. FUTURE APPLICATIONS

It must be clarified that the proposed analysis applies also for any type of sample that presents a linear elastic behaviour [31]. For example, the presented by this paper approach for the accurate determination of Young's modulus for big h/R ratios (Eq. 2.16) can be also used for the case of non-biological samples like the polyelectrolyte complex films [32] or polyelectrolyte multilayers [33]. As it has been previously reported, Polyelectrolyte multilayer films are frequently employed as a functional surface coating due to their stimuli responsiveness, and their electrical and mechanical properties [32]. The determination of their mechanical properties can be accurately performed using the analysis provided by this paper. However, it must be noted that biological samples are tested in a liquid environment and as result, adhesion forces are minimized. On the contrary, when non-biological samples are tested in ambient air conditions, the interaction between the AFM tip and the sample is affected by the humidity [34]. The tip-sample interaction is dominated by capillary forces (if the relative humidity is high), especially for hydrophilic surfaces [34]. The humidity of the environment can affect the Young's modulus measurements (a thin layer of humidity between the tip and the sample contributes to the interaction force). In this case, the provided by this paper theory combined with the theory of the geometric potential can be used [35-39]. The effects of the capillary forces can be easily determined in the aforementioned cases [35, 36]. In addition, another interesting application is the mechanical characterization of biological membranes on artificial surfaces. These biological membranes can be used as coatings for microcapsules. For example, the leucocyte cell membrane can be used for the modification of Janus microcapsules [40]. The mechanical characterization of the membrane can be performed using AFM and the related theory regarding the Young's modulus determination as it was previously presented in this paper.

CONCLUSION

In this paper, we present an analysis regarding the errors provided in spherical indentations for big h/R ratios. In addition, an equation which takes into account the relation between the indentation depth and the indenter's radius as a factor is presented. Despite the fact that the arising errors were not that extended, when combined to errors resulting from other parameters may lead to significant errors in the calculation of the Young's modulus values. Thus, significant research efforts should focus on the development of reliable theoretical tools and equations which can be applied generally without significant assumptions that may lead to false results.

CONSENT FOR PUBLICATION

Not applicable.

AVAILABILITY OF DATA AND MATERIALS

Not applicable.

FUNDING

None.

CONFLICT OF INTEREST

The authors declare no conflict of interest, financial or otherwise.

ACKNOWLEDGEMENTS

Declared none.

Appendix: Materials and Methods

Cell culturing: H4 human glioma cells (ATCC) were used for the evaluation of the proposed technique. The protocol used for the preparation of glioma cells has been previously reported by Kontomaris *et al.*, 2019 [24].

AFM experiments and analysis: A Molecular Imaging-Agilent PicoPlus AFM system (now known as AFM 5500 Keysight technologies) with a round (nominal value: 2.5 μm radius) ball-shape tip (CP-PNPL-BSG), and spring constant of 0.08 N/m was used for spherical indentation experiments. The spring's constant of the cantilever was determined using the thermal noise method. Curve fitting was performed using the Atomic J software [41].

REFERENCES

[1] Kontomaris, S.V.; Stylianou, A. Atomic force microscopy for university students: applications in biomaterials. *Eur. J. Phys.*, **2017**, *38*(3), 033003. http://dx.doi.org/10.1088/1361-6404/aa5cd6

[2] Alessandrini, A.; Facci, R. AFM: a versatile tool in biophysics. *Meas. Sci. Technol.*, **2005**, *16*, R65-R92. http://dx.doi.org/10.1088/0957-0233/16/6/R01

[3] Allison, D.P.; Mortensen, N.P.; Sullivan, C.J.; Doktycz, M.J. Atomic force microscopy of biological samples. *Wiley Interdiscip. Rev. Nanomed. Nanobiotechnol.,* **2010**, *2*(6), 618-634. http://dx.doi.org/10.1002/wnan.104

[4] Mateu, M.G. Mechanical properties of viruses analyzed by atomic force microscopy: a virological perspective. *Virus Res.*, **2012**, *168*(1-2), 1-22. http://dx.doi.org/10.1016/j.virusres.2012.06.008

[5] Pharr, G.M.; Oliver, W.C.; Brotzen, F.R. On the generality of the relationship among contact stiffness, contact area, and elastic modulus during indentation. *J. Mater. Res*., **1992**, *7*(3), 613-617. http://dx.doi.org/10.1557/JMR.1992.0613

[6] Oliver, W.C.; Pharr, G.M. Measurement of hardness and elastic modulus by instrumented indentation: Advances in understanding and refinements to methodology. *J. Mater. Res.*, **2004**, *19*(1), 3-20. http://dx.doi.org/10.1557/jmr.2004.19.1.3

[7] Darling, E.M. Force scanning: a rapid, high-resolution approach for spatial mechanical property mapping. *Nanotechnology*, **2011**, *22*(17), 175707. http://dx.doi.org/10.1088/0957-4484/22/17/175707

[8] Kurland, N.E.; Drira, Z.; Yadavalli, V.K. Measurement of nanomechanical properties of biomolecules using atomic force microscopy. *Micron*, **2012**, *43*(2-3), 116-128. http://dx.doi.org/10.1016/j.micron.2011.07.017

[9] Stylianou, A.; Kontomaris, S.V.; Yova, D. Assessing Collagen Nanoscale Thin Films Heterogeneity by AFM Multimode Imaging and Nanoindetation for NanoBioMedical Applications. *Micro Nanosyst*., **2014***, 6*(2), 95-102. http://dx.doi.org/10.2174/1876402906021411271144448

[10] Stylianou, A.; Yova, D.; Alexandratou, E. Investigation of the influence of UV irradiation on collagen thin films by AFM imaging. *Mater. Sci. Eng. C*, **2014**, *45*, 455-468. http://dx.doi.org/10.1016/j.msec.2014.09.006

[11] Kontomaris, S.V.; Yova, D.; Stylianou, A.; Politopoulos, K. The significance of the percentage differences of Young's modulus in the AFM nanoindentation procedure. *Micro Nanosyst.*, **2015**, *7*(2), 86-97. http://dx.doi.org/10.2174/1876402908666151111234441

[12] Kontomaris, S.V.; Stylianou, A.; Malamou, A.; Stylianopoulos, T. A discussion regarding the approximation of cylindrical and spherical shaped samples as half spaces in AFM nanoindentation experiments. *Mater. Res. Express*, **2018**, *5*(8), 085402 http://dx.doi.org/10.1088/2053-1591/aad2c9

[13] Kontomaris, S.V.; Malamou, A. An extension of the general nanoindentation equation regarding cylindrical – shaped samples and a simplified model for the contact ellipse determination. *Mater. Res. Express*, **2018**, *5*(12), 125403. http://dx.doi.org/10.1088/2053-1591/aae0bc

[14] Kontomaris, S.V.; Yova, D.; Stylianou, A.; Balogiannis, G. The effects of UV irradiation on collagen D-band revealed by atomic force microscopy. *Scanning*, **2015**, *37*(2), 101-111. http://dx.doi.org/10.1002/sca.21185

[15] Kontomaris, S.V.; Stylianou, A.; Malamou, A.; Nikita, K.S. An alternative approach for the Young's modulus determination of biological samples regarding AFM indentation experiments. *Mater. Res. Express*, **2018**, *6*(2), 025407. http://dx.doi.org/10.1088/2053-1591/aaef10

[16] Kontomaris, S.V. The hertz model in afm nanoindentation experiments: applications in biological samples and biomaterials. *Micro Nanosyst.,* **2018**, *10*(1), 11-22. http://dx.doi.org/10.2174/1876402910666180426114700

[17] Johnson, K.L.; Greenwood, J.A. An adhesion map for the contact of elastic spheres. *J. Colloid Interface Sci*., **1997**, *192*(2), 326-333. http://dx.doi.org/10.1006/jcis.1997.4984

[18] Johnson, K.; Kendall, K.; Roberts, A. Surface energy and the contact of elasticsolids. *Proc. R. Soc. Lond.*, **1971**, *324*, 301-313. http://dx.doi.org/10.1098/rspa.1971.0141

[19] Maugis, D. Adhesion of spheres: the JKR-DMT transition using a Dugdale model. J. *Colloid Interface Sci.*, **1992**, *150*(1), 243-269. http://dx.doi.org/10.1016/0021-9797(92)90285-T

[20] Persch, G.; Born, C.; Utesch, B. Nano-hardness investigations of thin films by an atomic force microscope. *Microelectron. Eng.*, **1994**, *24*(1-4), 113-121. http://dx.doi.org/10.1016/0167-9317(94)90061-2

[21] Radmacher, M. Studying the mechanics of cellular processes by atomic force microscopy. *Methods Cell Biol.*, **2007**, *83*, 347-372. http://dx.doi.org/10.1016/S0091-679X(07)83015-9

[22] Johnson, K.L. *Contact mechanics*; Cambridge University Press: Cambridge, **1985**. http://dx.doi.org/10.1017/CBO9781139171731

[23] Wenger, M.P.E.; Bozec, L.; Horton, M.A.; Mesquida, P. Mechanical properties of collagen fibrils. *Biophys. J*., **2007**, *93*(4), 1255-1263. http://dx.doi.org/10.1529/biophysj.106.103192

[24] Kontomaris, S.V.; Stylianou, A.; Nikita, K.S.; Malamou, A.; Stylianopoulos, T. A simplified approach for the determination of fitting constants in Oliver-Pharr method regarding biological samples. *Phys. Biol*., **2019**, *16*(5), 056003 http://dx.doi.org/10.1088/1478-3975/ab252e

[25] Guo, X.; Bonin, K.; Scarpinato, K.; Guthold, M. The effect of neighboring cells on the stiffness of cancerous and non-cancerous human mammary epithelial cells. *New J. Phys.*, **2014**, *16*(10), 105002. http://dx.doi.org/10.1088/1367-2630/16/10/105002

[26] Shimizu, Y.; Kihara, T.; Haghparast, S.M.; Yuba, S.; Miyake, J.; Miyake, J. Simple display system of mechanical properties of cells and their dispersion. *PLoS One*, **2012**, *7*(3), e34305. http://dx.doi.org/10.1371/journal.pone.0034305

[27] Grant, C.A.; Brockwell, D.J.; Radford, S.E.; Thomson, N.H. Tuning the elastic modulus of hydrated collagen fibrils. *Biophys. J.*, **2009**, *97*(11), 2985-2992. http://dx.doi.org/10.1016/j.bpj.2009.09.010

[28] Sajeesh, P.; Raj, A.; Dobleb, M.; Sen, A.K. Characterization and sorting of cells based on stiffness contrast in a microfluidic channel. *RSC Advances*, **2016**, *6*, 74704-74714. http://dx.doi.org/10.1039/C6RA09099K

[29] Andriotis, O.G.; Manuyakorn, W.; Zekonyte, J.; Katsamenis, O.L.; Fabri, S.; Howarth, P.H.; Davies, D.E.; Thurner, P.J. Nanomechanical assessment of human and murine collagen fibrils via atomic force microscopy cantilever-based nanoindentation. *J. Mech. Behav. Biomed. Mater.*, **2014**, *39*, 9-26. http://dx.doi.org/10.1016/j.jmbbm.2014.06.015

[30] Heim, A.J.; Matthews, W.G.; Koob, T.J. Determination of the elastic modulus of native collagen fibrils via radial indentation. *Appl. Phys. Lett.*, **2006**, *89*(18), 181902. http://dx.doi.org/10.1063/1.2367660

[31] Kontomaris, S.V.; Stylianou, A.; Nikita, K.S.; Malamou, A. Determination of the linear elastic regime in AFM nanoindentation experiments on cells. *Mater. Res. Express*, **2019**, *6*(11), 115410. http://dx.doi.org/10.1088/2053-1591/ab4f42

[32] Gai, M.; Frueh, J.; Kudryavtseva, V.L.; Mao, R.; Kiryukhin, M.V.; Sukhorukov, G.B. Patterned microstructure fabrication: polyelectrolyte complexes vs polyelectrolyte multilayers. *Sci. Rep.*, **2016**, *6*, 37000. http://dx.doi.org/10.1038/srep37000

[33] Gai, M.; Frueh, J.; Kudryavtseva, V.L.; Yashchenok, A.M.; Sukhorukov, G.B. Polylactic acid sealed polyelectrolyte multilayer microchambers for entrapment of salts and small hydrophilic molecules precipitates. *ACS Appl. Mater. Interfaces*, **2017**, *9*(19), 16536-16545. http://dx.doi.org/10.1021/acsami.7b03451

[34] Seppä, J.; Reischl, B.; Sairanen, H.; Korpelainen, V.; Husu, H.; Heinonen, M.; Raiteri, P.; Rohl, A.L.; Nordlund, K.; Lassila, A. Atomic force microscope adhesion measurements and atomistic molecular dynamics simulations at different humidities. *Meas. Sci. Technol*., **2017**, *28*(3), 034004, http://dx.doi.org/10.1088/1361-6501/28/3/034004

[35] Liu, P.; He, J.H. Geometric potential: An explanation of nanofiber's wettability. *Therm. Sci.*, **2017**, *22*(1), 146-146.

[36] Li, X.X.; He, J.H. Nanoscale adhesion and attachment oscillation under the geometric potential. Part 1: The formation mechanism of nanofiber membrane in the electrospinning. *Results Phys*, **2019**, *12*, 1405-1410. http://dx.doi.org/10.1016, /j.rinp.2019.01.043

[37] He, J.H. A Note on Elementary Cobordism and Negative Space. *Int. J. Nonlin. Sci. Num.*, **2010**, *11*(12), 1093-1095. http://dx.doi.org/10.1515/IJNSNS.2010.11.12.1093

[38] He, J.H. Frontier of Modern Textile Engineering and Short Remarks on Some Topics in Physics. *Int. J. Nonlin. Sci. Num.*, **2010**, *11*(7), 555-563. http://dx.doi.org/10.1515/IJNSNS.2010.11.7.555

[39] He, J.H. Inverse Problems of Newton's Laws. *Int. J. Nonlin. Sci. Num.*, **2009**, *10*(9), 1087-1091. http://dx.doi.org/10.1515/IJNSNS.2009.10.9.1087

[40] He, W.; Frueh, J.; Wu, Z.; He, Q. How Leucocyte Cell Membrane Modified Janus Microcapsules are Phagocytosed by Cancer Cells. *ACS Appl. Mater. Interfaces*, **2016**, *8*(7), 4407-4415. http://dx.doi.org/10.1021/acsami.5b10885 PMID: 26824329

[41] Hermanowicz, P.; Sarna, M.; Burda, K.; Gabryś, H. AtomicJ: an open source software for analysis of force curves. *Rev. Sci. Instrum.*, **2014**, *85*(6), 063703. http://dx.doi.org/10.1063/1.4881683